

## LncRNA XIST promotes adjuvant-induced arthritis by increasing the expression of YY1 via miR-34a-5p

Yazhi Wei<sup>1</sup> , Liping Dai<sup>2</sup> , Yanqun Deng<sup>1</sup> , Zhizhong Ye<sup>2</sup> <sup>1</sup>Department of Clinical Laboratory, Shenzhen Futian Hospital for Rheumatic Diseases, Shenzhen, Guangdong, China<sup>2</sup>Department of Rheumatology and Immunology, Shenzhen Futian Hospital for Rheumatic Diseases, Shenzhen, Guangdong, China

### ABSTRACT

**Objectives:** This study aims to explore the mechanism by which long non-coding ribonucleic acids (lncRNA) X-inactive specific transcript (XIST) affects the progression of adjuvant-induced arthritis (AIA).

**Materials and methods:** Freund's complete adjuvant was used to induce arthritis in rats. The polyarthritis, spleen and thymus indexes were calculated to evaluate AIA. Hematoxylin-eosin (H&E) staining was used to reveal the pathological changes in the synovium of AIA rats. Enzyme-linked immunosorbent assay (ELISA) was performed to detect the expression of tumor necrosis factor- $\alpha$  (TNF- $\alpha$ ), interleukin (IL)-6 and IL-8 in the synovial fluid of AIA rats. The cell continuing kit (CCK)-8, flow cytometry, and Transwell assays were used to assess the proliferation, apoptosis, migration and invasion of transfected fibroblast-like synoviocytes (FLS) isolated from AIA rats (AIA-FLS). Dual-luciferase reporter assay was performed to verify the binding sites between XIST and miR-34b-5p or between YY1 mRNA and miR-34b-5p.

**Results:** The XIST and YY1 were highly expressed, and miR-34a-5p was lowly expressed in the synovium of AIA rats and in AIA-FLS. Silencing of XIST impaired the function of AIA-FLS *in vitro* and inhibited the progression of AIA *in vivo*. The XIST promoted the expression of YY1 by competitively binding to miR-34a-5p. Inhibition of miR-34a-5p strengthened the function of AIA-FLS by upregulating XIST and YY1.

**Conclusion:** The XIST controls the function of AIA-FLS and may promote the progression of rheumatoid arthritis via the miR-34a-5p/YY1 axis.

**Keywords:** Adjuvant-induced arthritis, fibroblast-like synoviocytes, LncRNA XIST, miR-34a-5p, Yin Yang 1.

Rheumatoid arthritis (RA) is a chronic, systemic inflammatory disease mostly manifested by symmetrical pain and swelling of multiple joints (polyarthritis) and it can also present as monoarthritis or oligoarthritis.<sup>1</sup> Genetic factors contribute to a significant portion of the risk of RA, although the disease progression can be influenced by epigenetic modifications and interactions between genes and environment.<sup>2</sup> Rheumatoid arthritis predominantly affects middle-aged populations and exhibits a three-fold higher

frequency in women than men.<sup>3</sup> Patients with RA can also present with extra-articular manifestations such as interstitial lung disease, cervical spine disease and cardiovascular events.<sup>4-6</sup> Early diagnosis and interventions using disease-modifying antirheumatic drugs (DMARDs) greatly increase the chance of remission in patients with RA and prevent subsequent irreversible disability.<sup>7</sup> Despite the improvement of outcomes and availability of biologic therapies, there is still an unmet need in the treatment of RA with refractoriness.<sup>8</sup>

**Received:** September 27, 2021 **Accepted:** February 21, 2022 **Published online:** June 27, 2022

**Correspondence:** Zhizhong Ye, MD. Department of Rheumatology and Immunology, Shenzhen Futian Hospital for Rheumatic Diseases, No. 22 Nonglin Road, Futian District, Shenzhen, Guangdong 518040, P.R. China.  
E-mail: yezhizhong20@163.com

### Citation:

Wei Y, Dai Y, Deng Y, Ye Z. LncRNA XIST promotes adjuvant-induced arthritis by increasing the expression of YY1 via miR-34a-5p. Arch Rheumatol 2023;38(1):82-94.

©2023 Turkish League Against Rheumatism. All rights reserved.

This is an open access article under the terms of the Creative Commons Attribution-NonCommercial License, which permits use, distribution and reproduction in any medium, provided the original work is properly cited and is not used for commercial purposes (<http://creativecommons.org/licenses/by-nc/4.0/>).

Long non-coding ribonucleic acids (RNAs; lncRNAs) are important players in gene expression, RNA metabolism and epigenetic remodeling and, therefore, control diverse cellular activities, as well as embryonic development.<sup>9</sup> Increasing studies have revealed the involvement of lncRNAs in RA. To illustrate, the lncRNA PICSAR was upregulated in RA and promoted the proliferation, migration and invasion of inflammatory fibroblast-like synoviocytes (FLS).<sup>10</sup> The FLS, residing in the synovial intimal lining, acquire invasiveness during RA and produce inflammatory cytokines and proteases to destroy cartilage.<sup>11</sup> Silencing of lncRNA X-inactive specific transcript (XIST) has been reported to suppress inflammatory response and promote differentiation in RA osteoblasts,<sup>12</sup> but whether XIST regulates the function of FLS is unknown.

The lncRNAs are recognized as positive regulators of gene expression by sequestering microRNAs (miRNAs) from their target messenger RNAs (mRNAs).<sup>13</sup> The miRNAs induce silencing of target genes through complementary binding of the seed region to the 3' untranslated region (3'UTR) of mRNAs.<sup>14</sup> Yin Yang 1 (YY1) is a transcription factor exhibiting promotive effect in RA by stimulating interleukin (IL)-6-induced T-helper 17 (Th17) differentiation.<sup>15</sup> Upregulation of YY1 was also detected in RA-FLS where it was targeted by miR-410-3p.<sup>16</sup> In a recent report, YY1 was targeted by miR-34a-5p in regulating the proliferation and invasion of hepatocellular carcinoma cells.<sup>17</sup> Song et al.<sup>18</sup> found that miR-34a-5p inhibited the proliferation and inflammatory response of RA-FLS by decreasing the expression of XBP1. It is likely that miR-34a-5p mediates FLS function partially through interaction with YY1. A previous study showed that miR-34a-5p was a target of XIST in regulating the malignant potential of pancreatic cancer cells.<sup>19</sup> Based on the above evidence, we hypothesized that XIST might promote RA by regulating the miR-34a-5p/YY1 axis in FLS. This study aims to validate the hypothetical axis regulated by XIST and add confidence to targeted therapies for RA.

## MATERIALS AND METHODS

### Model establishment

Twenty-four male Wistar rats (6-week-old, 150±20 g, Hunan SJA Laboratory Animal Co.,

Ltd., Hunan, China) were used for establishment of an adjuvant-induced arthritis (AIA) model.

The AIA model was established using the methods presented in a previous study.<sup>20</sup> After one week adaptation to the experimental environments, 18 rats were randomly selected and given intradermal injection of Freund's complete adjuvant F5881 (1 µL/g, Sigma-Aldrich, St. Louis, MI, USA) in the toes of the left hind limbs. The remaining six rats were assigned to normal group and injected with an equal amount of normal saline. The 18 rats were assigned to AIA, AIA + sh-NC, and AIA + sh-XIST groups (n=6 per group). The AIA + sh-NC group was injected with negative control lentiviruses through tail vein. The AIA + sh-XIST group was injected with 100 pmol XIST silencing lentiviruses.<sup>21</sup>

We first estimated the sample size using the G\*Power version 3.1.9.2 (Heinrich-Heine-Universität, Düsseldorf, Düsseldorf, Germany) before the experiments. The analysis showed that a sample size of six was sufficient. As the main purpose of the experiments was to determine whether there were significant differences between the experimental groups, we also used another method mentioned in a previous study<sup>22</sup> to calculate the sample size. The resource equation method<sup>23,24</sup> was also used to determine the sample size. Briefly, an "E" value was measured, which represented the degree of freedom in analysis of variance (ANOVA). If E was less than 10, more animals were needed to increase the chance of getting a more significant result. If E was greater than 20, more animals would not increase the chance of getting a significant result. This method was based on ANOVA and applicable to all animal experiments. Any sample size could be considered sufficient as long as the E value was between 10 and 20. The E value was calculated by the following formula:  $E = \text{total number of animals} - \text{total number of groups}$ . The sample size used in this study had an E value between 10 and 20. Therefore, we believed that this sample size (n=6) was reasonable and sufficient.

### Polyarthritis score

The rats were scored at Weeks 1, 2, 3, and 4 after the injection according to the following criteria: 0= no swelling; 1= toe swelling; 3= swelling of the paw under the ankle; 4=

swelling of the whole paw including the ankle. A sum of the scores of four limbs was recorded as the final result, with a maximum value of 1220.

### Splenic and thymic indexes

The rats were euthanatized by an overdose of pentobarbital sodium (160 mg/kg) four weeks after the model establishment.<sup>25</sup> The spleen and thymus of the rats were extracted and weighed. The spleen (or thymus) index = spleen weight (or thymus weight)/body weight. Also, the synovium of the right hind limb and synovial fluid were collected from the rats.

### Hematoxylin and eosin (H&E) staining

The synovial tissues were embedded and continuously sliced. The slices (4  $\mu$ m) were spread and attached to slides in 46°C water. Then, the slices were baked for 2 h and chilled for 10 min. The slides were sequentially immersed in the following solutions: xylene I (10 min), xylene II (10 min), absolute ethanol I (5 min), absolute ethanol II (5 min), 90% ethanol (2 min), 80% ethanol (2 min), 70% ethanol (2 min), running water (5 min), hematoxylin solution (5 ~ 10 min), running water (5 min), hydrochloric acid-ethanol (2~3 sec), running water (5 min), lithium carbonate solution (10 min), running water (10 min), eosin solution (2 min), running water (5 min), 80% ethanol (2 min), 90% ethanol (2 min), absolute ethanol (2 min), and xylene (2 min). The slides were wiped and mounted with neutral balsam before microscopy.

### Enzyme-linked immunosorbent assay (ELISA)

The expression of inflammatory cytokines tumor necrosis factor-alpha (TNF- $\alpha$ ), IL-6, and IL-8 in the synovial fluid was detected using TNF- $\alpha$  ELISA kit (96T), IL-6 ELISA kit (96T), and IL-8 ELISA kit (96T) (all from Dakewe Biotech Co., Ltd., Shenzhen, China). Briefly, 100  $\mu$ L of samples were incubated with biotinylated antibody working solution (1:100, 100  $\mu$ L/well) for 2 h and the absorbance was read at 450 nm. The experiment was repeated three times.

### Quantitative real-time polymerase chain reaction (qRT-PCR)

Total RNA was extracted using TRIzol reagent (Invitrogen, Carlsbad, CA, USA) and reverse transcribed into cDNA using PrimeScript RT kit (RR037A, Takara, Tokyo, Japan). The miRcute Plus miRNA first-strand cDNA synthesis kit (TIANGEN Biotech Co., Ltd., Beijing, China) was used to synthesize miRNA cDNA from the total RNA. Samples were analyzed by the ABI 7500 real-time PCR system (Applied Biosystems, Foster City, CA, USA) according to the instructions of SYBR® Premix Ex Taq™ II Kit (RR820A, Takara, Tokyo, Japan). The glyceraldehyde 3-phosphate dehydrogenase (GAPDH) or U6 was used as an internal reference. Each group was tested three times. The 2- $\Delta\Delta$ Ct method<sup>26</sup> was used to calculate the relative expression of each target gene ( $\Delta\Delta$ Ct=  $\Delta$ Ct experimental group- $\Delta$ Ct control group,  $\Delta$ Ct= Ct target gene-Ct internal

**Table 1.** Primer sequences

Primer	Sequence
miR-34a-5p-F	5'-CGCGTGGCAGTGTCTTAGCT-3'
miR-34a-5p-R	5'-AGTGCCAGGGTCCGAGGTATT-3'
U6-F	5'-CTCGCTTCGGCAGCACA-3'
U6-R	5'-AACGCTTCACGAATTTGCGT-3'
XIST-F	5'-AACCACCACACGTCAAGCTCTTC-3'
XIST-R	5'-AGTGCCAGGCATGTTGATCTTCAG-3'
GAPDH-F	5'-AATCCCATCACCATCTTC-3'
GAPDH-R	5'-AGGCTGTTGTCATACTTC-3'

F: Forward; R: Reverse; XIST: X-inactive specific transcript.

control). Primers used in the PCR were designed by Sangon Biotech Co., Ltd. (Shanghai, China) and listed in Table 1.

### **Isolation and culture of rat FLS**

The synovial tissues were digested with trypsin. Isolated FLS were passaged for three generations. Cells collected from the normal rats were named as FLS group, and those from the model rats were named as AIA-FLS. FLS or AIA-FLS (at the logarithmic growth phase) were suspended in Dulbecco's modified eagle medium (DMEM) containing 10% fetal bovine serum (FBS) and cultured in a 24-well plate ( $1 \times 10^5$  cells/well) at 37°C with 5% carbon dioxide (CO<sub>2</sub>) and 95% humidity.

### **Lentiviral transduction**

Lentiviral plasmids carrying miR-34a-5p mimic, mimic negative control (NC), XIST shRNA (sh-XIST), sh-NC, YY1 overexpression vector (oe-YY1) or oe-NC, as well as virus packaging kits were purchased from GeneCopoeia (Rockville, MD, USA). The miR-34a-5p inhibitor and inhibitor NC were purchased from GenePharma (Shanghai, China). The HEK293T cells were transfected and after 48 h, the virus titer was obtained using a p24 ELISA kit (Cell Biolabs, Inc., San Diego, CA, USA). The AIA-FLS were infected with the prepared lentiviruses for 24 h and, then, cultured for another 48 h. Stable cell lines were selected using puromycin (P8230, Solarbio Science & Technology Co., Ltd., Beijing, China) and the transfection effectiveness was evaluated using qRT-PCR.

### **Cell continuing kit (CCK)-8 assay**

Diluted suspension of transfected AIA-FLS ( $1 \times 10^6$  cells/mL, 100  $\mu$ L per well) was added into a 96-well plate (each group used three wells). Each well was added with 10  $\mu$ L of CCK-8 reagent (Dojindo Molecular Technologies Inc., Tokyo, Japan) after the cells were incubated for 24, 48, and 72 h. After another 2 h of incubation, the absorbance was read at 450 nm. The assay was repeated three times.

### **Flow cytometry**

Transfected AIA-FLS were cultured for 48 h (37°C, 5% CO<sub>2</sub>), washed three times with PBS, and suspended with 0.5 mL of binding buffer. The cells were incubated with 6  $\mu$ L of Annexin V-FITC and 20  $\mu$ L of PI solutions (V13242, Thermo Fisher Scientific, Waltham,

MA, USA) at room temperature away from light for 15 min. The mixture was centrifuged and the cell pellets were resuspended with 300  $\mu$ L of binding buffer. The apoptosis rate was measured by a flow cytometer (Attune NxT, Thermo Fisher Scientific) and averaged from three independent experiments.

### **Transwell assay**

Matrigel (Qcbio Science&Technologies Co., Ltd., Shanghai, China) cryopreserved at -20°C was thawed at 4°C and diluted with serum-free medium at 1:4. Each Transwell insert was coated with 30  $\mu$ L of Matrigel and incubated with a 24-well plate overnight (37°C, 5% CO<sub>2</sub>). Transfected AIA-FLS were suspended with DMEM containing 1% bovine serum albumin (BSA). The apical chamber of each Transwell was added with 100  $\mu$ L of cell suspension ( $1 \times 10^6$  cells/mL), and the basolateral chamber was added with 500  $\mu$ L of DMEM medium containing 20% FBS. The cells were cultured under standard conditions for 48 h, after which the culture medium in both the apical and basolateral chambers was discarded. Cells remaining on the upper surface of the permeable membrane were wiped off with a cotton swab. The basolateral chamber was added with 500  $\mu$ L of PBS, and the PBS was gently flapped to clean the lower surface of the membrane. The cleaning was repeated once. The permeable membrane was soaked in 500  $\mu$ L of 4% paraformaldehyde in the basolateral chamber for 20 min. Then the fixative was discarded and the Transwell insert was inverted to allow the membrane air dry. The lower surface of the membrane was stained with DAPI away from light for 2 min and, then, washed with PBS. Matrigel-coated Transwell inserts were used for analysis of invasion and uncoated Transwell inserts were used for analysis of migration. Five fields in each membrane were randomly selected for cell counting. Each assay was repeated three times.

### **Western blotting**

Cells were collected by trypsin digestion and lysed with enhanced RIPA buffer (Boster, Wuhan, China) containing protease inhibitors. The concentration of protein was determined using a BCA kit (Boster). Proteins were separated by 10% SDS-PAGE and electroblotted onto a polyvinylidene fluoride (PVDF) membrane. Unoccupied binding sites on the membrane were

blocked by 5% BSA at room temperature for 2 h. The membrane was incubated with diluted YY1 antibody (ab109237, 1:1000, Abcam, Cambridge, UK) and GAPDH antibody (ab8245, 1:5000, Abcam) at 4°C overnight. After washes, the membrane was incubated with HRP-labeled goat anti-rabbit secondary antibody (ab6721, 1:2000, Abcam) at room temperature for 1 h. Then, the membrane was incubated with enhanced chemiluminescence (ECL) working solution (EMD Millipore, Burlington, MA, USA) at room temperature for 1 min and excess ECL solution was removed. The membrane was sealed with a plastic wrap and placed in a dark cassette. An X-ray film was put on the top of the membrane and exposed for 5 to 10 min. The bands were quantified by Image J (National Institutes of Health) with GAPDH used as an internal control. Each group was tested three times.

### Dual-luciferase reporter assay

The binding sites between XIST and miR-34a-5p were predicted by starBase (<http://starbase.sysu.edu.cn/starbase2/index>.

php). The binding sites between miR-34a-5p and YY1 mRNA were predicted by TargetScan ([http://www.targetscan.org/vert\\_71/](http://www.targetscan.org/vert_71/)). XIST 3'UTR and YY1 3'UTR fragments complementary to the seed sequence of miR-34a-5p were synthesized according to the predicted binding sites. Mutations were designed based on the wild-type (WT) XIST and YY1. The WT or mutant-type (MUT) fragments were digested with restriction enzymes and inserted by T4 DNA ligase into pMIR-reporter plasmids (Promega, Madison, WI, USA). The plasmids were co-transfected with miR-34a-5p mimic or mimic NC into HEK-293T cells (Shanghai Beinuo Biotechnology Co., Ltd., Shanghai, China). The cells were collected and lysed 48 h after the transfection, and centrifuged for 3 to 5 min. The supernatant was taken for analysis of luciferase activity (Dual-Luciferase® Reporter Assay System, Promega). The relative luciferase activity was presented as the ratio of target luciferase activity/reference luciferase activity that was measured by a luminometer (Promega). Three independent experiments were done for this assay.

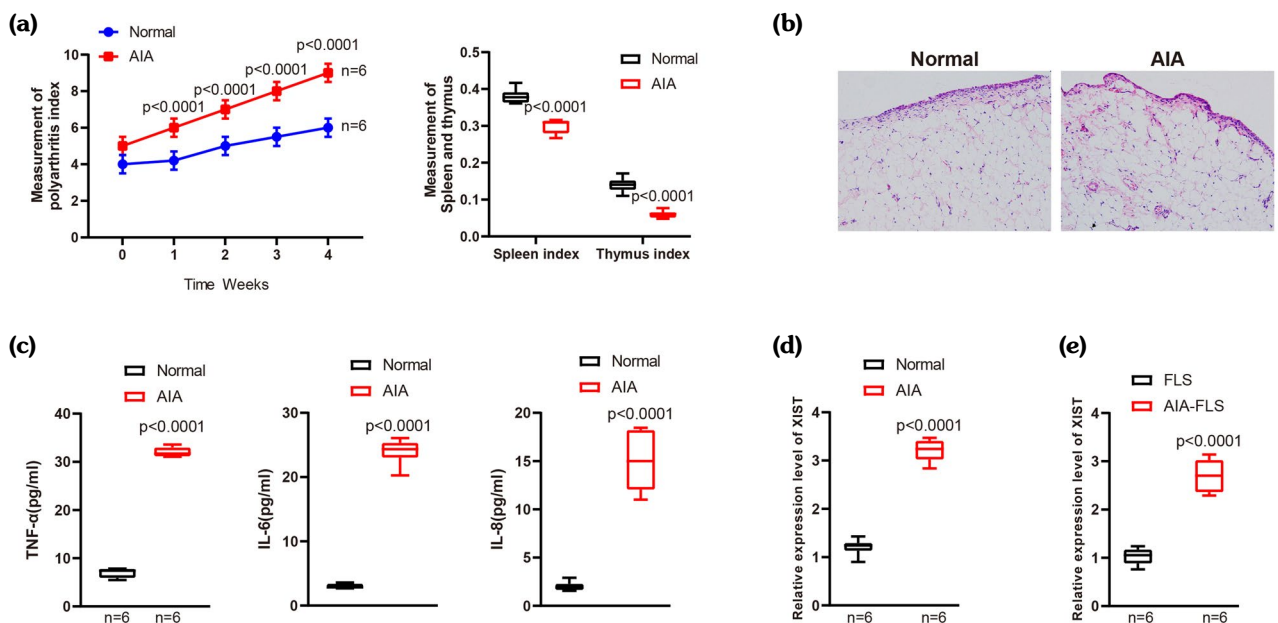


**Figure 1.** XIST is highly expressed in AIA. **(a)** The polyarthritis, spleen and thymus indexes were used to assess synovial inflammation in AIA rats. **(b)** H&E staining was used to reveal the histopathological changes in synovium. **(c)** ELISA was used to detect the expression of TNF- $\alpha$ , IL-6 and IL-8 in synovial fluid. qRT-PCR was to detect the expression of XIST in synovium **(d)** and in FLS and AIA-FLS **(e)**. Two-way analysis of variance was used to determine the p values in panel A. Student's t-test was used to determine the p values in panels C and D. Mann-Whitney U test was used to determine the p value in panel E. There were 6 rats in each group.

XIST: X-inactive specific transcript; AIA: Adjuvant-induced arthritis; TNF- $\alpha$ : Tumor necrosis factor-alpha; IL: Interleukin; qRT-PCR: Quantitative real-time polymerase chain reaction; FLS: Fibroblast-like synoviocytes.

## Statistical analysis

Statistical analysis was performed using the IBM SPSS version 21.0 software (IBM Corp., Armonk, NY, USA). Data were expressed in mean  $\pm$  standard deviation (SD). Two groups were compared by the t-test of normally distributed data or by the Mann-Whitney U test of non-normally distributed data. One-way ANOVA was used for multigroup comparisons. Two-way ANOVA was used for comparisons of groups at different time points. The Fisher's least significant difference test was applied for post-hoc multiple comparisons. A  $p$  value of  $<0.05$  was considered statistically significant.

## RESULTS

### XIST was highly expressed in AIA

An AIA model was established for studying the effect of XIST on AIA. The AIA group ( $n=6$ ) showed an increase in the polyarthrit

score (paw swelling) and decreases in the spleen and thymus indexes (Figure 1a, *vs.* the normal group,  $p<0.0001$ ). Moreover, the AIA group had distinct synovial hyperplasia and inflammatory cell infiltration in the synovium (Figure 1b, *vs.* the normal group). The results of ELISA showed that the expression of TNF- $\alpha$ , IL-6, and IL-8 in the synovial fluid of the AIA group was higher than that of the normal group (Figure 1c,  $p<0.0001$ ). Collectively, the above results indicated successful establishment of the AIA model. The qRT-PCR detection showed that the AIA group had a higher expression of XIST in the synovium than the normal group (Figure 1d,  $p<0.0001$ ). The expression of XIST was also increased in AIA-FLS compared to FLS (Figure 1e,  $p<0.0001$ ).

### Silencing of XIST inhibited proliferation, migration and invasion and promoted apoptosis in AIA-FLS

We silenced XIST in AIA-FLS to investigate the effect of XIST on FLS function in the AIA

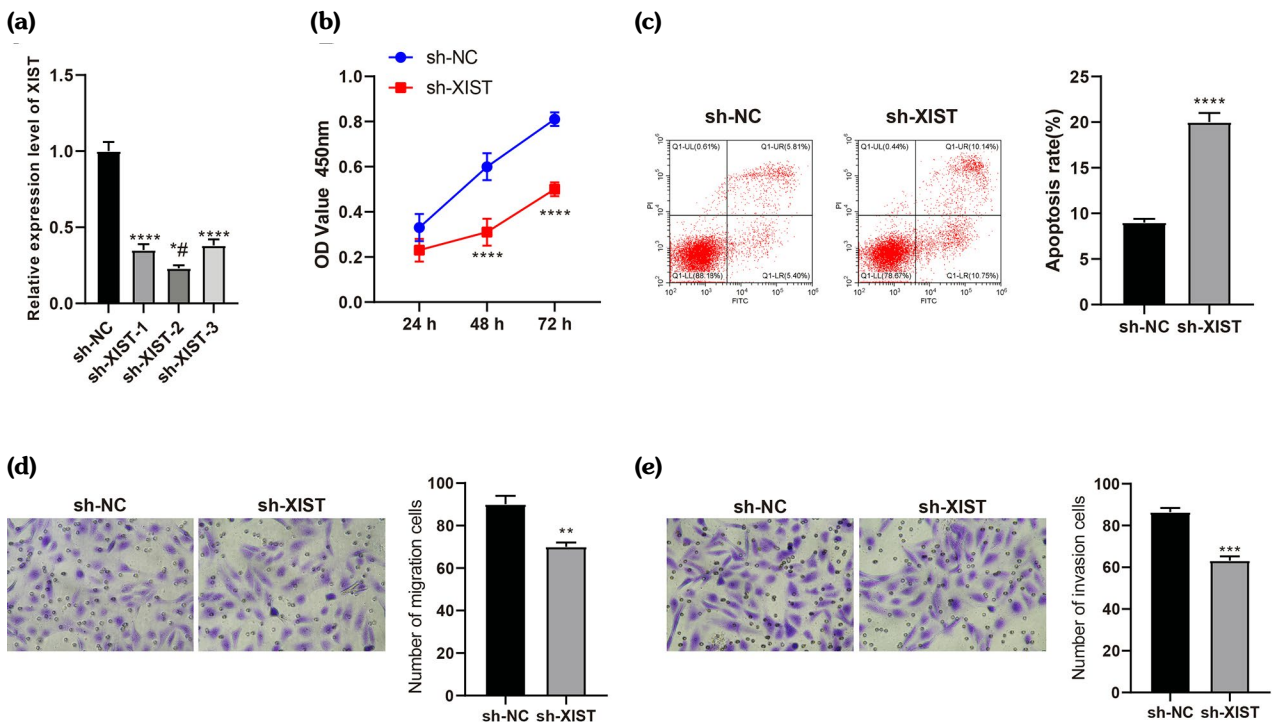


**Figure 2.** Silencing of XIST inhibits proliferation, migration and invasion and promotes apoptosis in AIA-FLS. AIA-FLS were transfected with sh-XIST or sh-NC. **(a)** qRT-PCR was used to analyze the silencing efficiencies of sh-XIST-1, sh-XIST-2 and sh-XIST-3. The CCK-8 assay, flow cytometry and Transwell assay were used to assess the proliferation **(b)**, apoptosis **(c)**, migration **(d)** and invasion **(e)** of AIA-FLS.

XIST: X-inactive specific transcript; \*\*\*\*  $p<0.0001$ , compared with the sh-NC group; ####  $p<0.0001$ , compared with the sh-XIST-1 and sh-XIST-3 groups. The above measurement data are expressed as mean  $\pm$  standard deviation. Independent samples t-test was performed for comparisons between two groups unless specifically stated. One-way analysis of variance was used for comparisons among multiple groups. Two-way analysis of variance was used to determine the  $p$  values in panel B. Each experiment was repeated three times; AIA: Adjuvant-induced arthritis; FLS: Fibroblast-like synoviocytes; sh-NC: Negative control short hairpin RNA; qRT-PCR: Quantitative real-time polymerase chain reaction; CCK: Cell continuing kit.

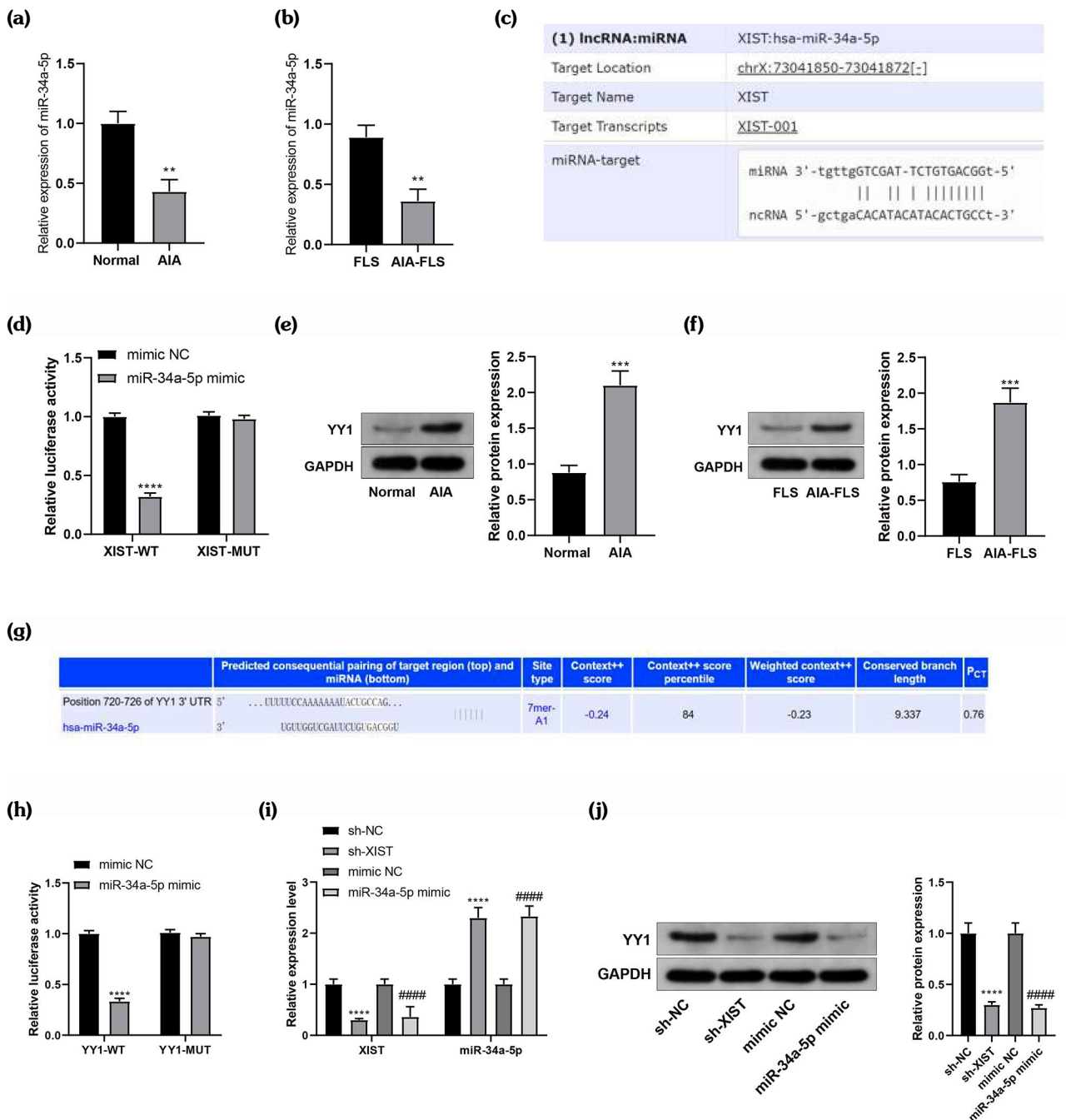


**Figure 3.** XIST promotes the expression of YY1 by competitively sponging miR-34a-5p. qRT-PCR was used to detect the expression of miR-34a-5p in the synovium of AIA rats **(a)** and in FLS and AIA-FLS **(b)**. **(c)** StarBase predicted the binding sites between XIST and miR-34a-5p. **(d)** Dual-luciferase assay was performed to verify the binding between XIST and miR-34a-5p. Western blotting was used to detect the expression of YY1 protein in the synovium of AIA rats **(e)** and in FLS and AIA-FLS **(f)**. **(g)** TargetScan predicted the binding sites between miR-34a-5p and YY1 mRNA. **(h)** Dual-luciferase assay was performed to verify the binding between miR-34a-5p and YY1 mRNA. **(i)** qRT-PCR was used to detect the expression of XIST and miR-34a-5p in cells transfected with sh-XIST or miR-34a-5p mimic. **(j)** Western blotting was used to detect the expression of YY1 protein in cells transfected with sh-XIST or miR-34a-5p mimic.

XIST: X-inactive specific transcript; \*\*\*\*  $p < 0.0001$ , compared with the Normal, FLS, sh-NC, mimic NC + XIST-WT or mimic NC + YY1-WT group. ####  $p < 0.05$ , compared with the mimic NC group. The above measurement data are expressed as mean  $\pm$  standard deviation. Independent samples t-test was performed for comparisons between two groups. One-way analysis of variance was used for comparisons among multiple groups. Each experiment was repeated three times. AIA, adjuvant-induced arthritis; FLS, fibroblast-like synoviocytes; qRT-PCR: Quantitative real-time polymerase chain reaction; AIA: Adjuvant-induced arthritis; FLS: Fibroblast-like synoviocytes; mRNA: Messenger ribonucleic acid; sh-NC: Negative control short hairpin RNA.

model. Compared to the sh-NC group, the expression of XIST was significantly decreased in the sh-XIST-1, sh-XIST-2 and sh-XIST-3 groups; among them, the sh-XIST-2 group showed the highest silencing efficiency (Figure 2a,  $p < 0.0001$ ). Therefore, sh-XIST-2 was selected for the following experiments. The results of CCK-8,

flow cytometry and Transwell assays showed that silencing of XIST inhibited proliferation (Figure 2b,  $p < 0.0001$ , vs. the sh-NC group), migration (Figure 2D,  $p = 0.0015$ , vs. the sh-NC group) and invasion (Figure 2e,  $p = 0.0002$ , vs. the sh-NC group) and promoted apoptosis (Figure 2c,  $p < 0.0001$ , vs. the sh-NC group) in AIA-FLS.

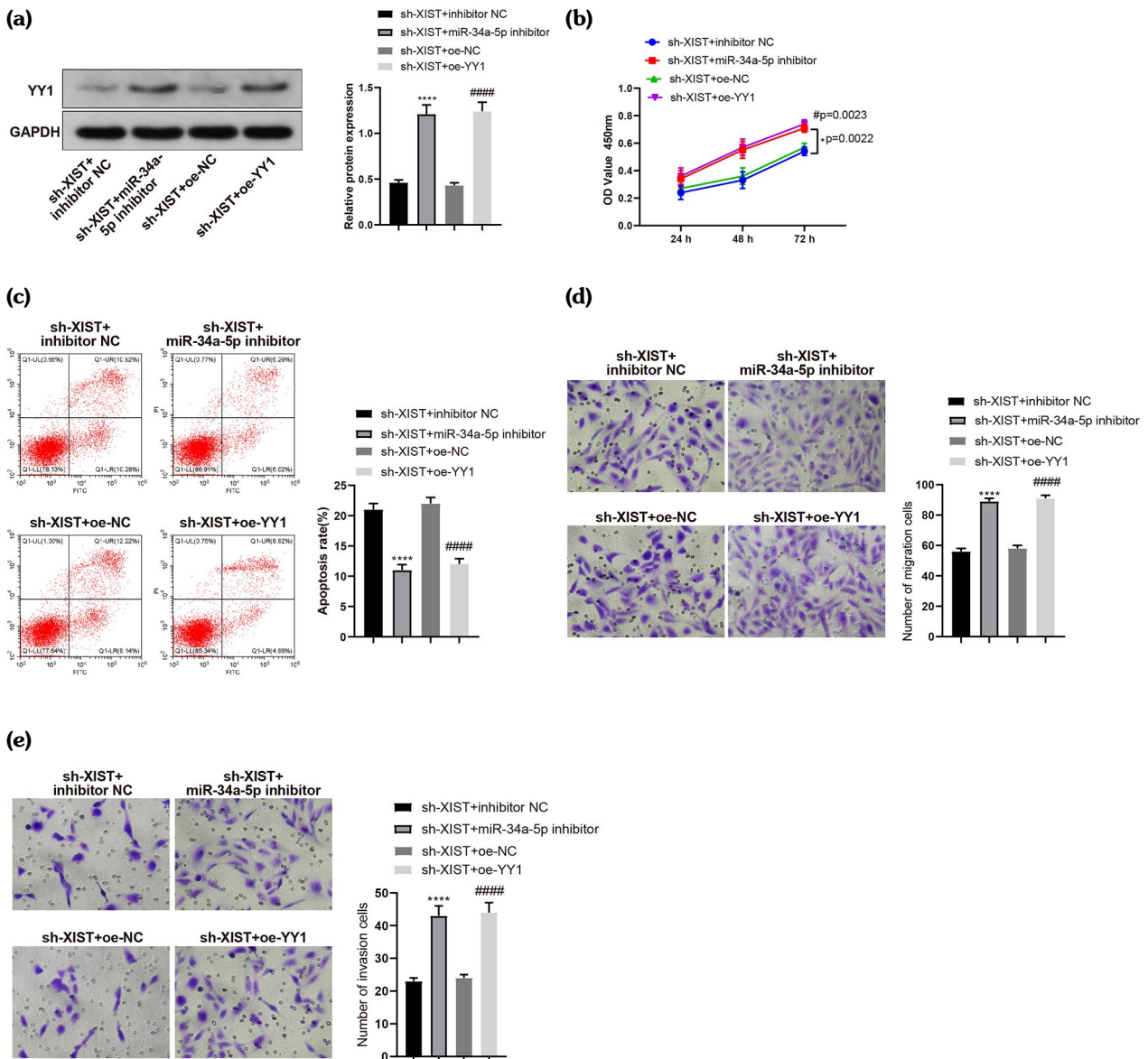


**Figure 4.** XIST regulates AIA-FLS function via miR-34a-5p/YY1 axis. AIA-FLS were transfected with sh-XIST + inhibitor NC, sh-XIST + miR-34a-5p inhibitor, sh-XIST + oe-NC or sh-XIST + oe-YY1. **(a)** Western blotting was used to detect YY1 protein. CCK-8, flow cytometry and Transwell assays were used to assess the proliferation **(b)**, apoptosis **(c)**, migration **(d)** and invasion **(e)** of AIA-FLS.

XIST: X-inactive specific transcript; \*\*\*\*  $p < 0.0001$ , compared with the sh-XIST + inhibitor NC group; ####  $p < 0.0001$ , compared with the sh-XIST + oe-NC group. The above measurement data are expressed as mean  $\pm$  standard deviation. Independent samples t-test was performed for comparisons between two groups unless specifically stated. One-way analysis of variance was used for comparisons among multiple groups. Two-way analysis of variance was used to determine the p values in panel B. Each experiment was repeated three times; AIA: Adjuvant-induced arthritis; FLS: Fibroblast-like synoviocytes; oe-NC: Negative control overexpression plasmid; oe-YY1: YY1 overexpression plasmid; CCK: Cell continuing kit.

### XIST promoted the expression of YY1 by competitively sponging miR-34a-5p

The expression of miR-34a-5p was significantly reduced in the synovium of the AIA group (Figure 3a,  $p=0.0022$ , *vs.* the normal group) and in AIA-FLS (Figure 3b,  $p=0.0029$ , *vs.* the FLS group). The public database starBase (<http://starbase.sysu.edu.cn/starbase2/index.php>) was used to predict the target genes of XIST. The analysis of the starBase data showed that miR-34a-5p could bind the 3'UTR of XIST (Figure 3c), and the luciferase reporter vectors were designed and used to verify the binding. Compared to the mimic NC group, cells transfected with miR-34a-5p mimic + XIST-WT showed a reduction in the luciferase activity ( $p<0.0001$ ), while cells transfected with XIST-MUT had no significant change in the luciferase activity (Figure 3d).

The Western blot analysis showed that the expression of YY1 was significantly increased in the synovium of the AIA group (Figure 3e,  $p=0.0007$ , *vs.* the normal group)

and in AIA-FLS (Figure 3f,  $p=0.001$ , *vs.* the FLS group). The predicted binding sites between miR-34a-5p and YY1 mRNA are presented in Figure 3g. Compared to the mimic NC group, cells transfected with miR-34a-5p mimic + YY1-WT showed a reduction in the luciferase activity ( $p<0.0001$ ), while cells transfected with YY1-MUT had no significant change in the luciferase activity (Figure 3h).

The XIST was downregulated ( $p<0.0001$ ) and miR-34-5p was upregulated ( $p<0.0001$ ) in cells transfected with sh-XIST or miR-34a-5p mimic (Figure 3i, *vs.* the sh-NC or mimic NC group). The expression of YY1 was significantly reduced in cells transfected with sh-XIST or miR-34a-5p mimic (Figure 3j,  $p<0.0001$ , *vs.* the sh-NC or mimic NC group). Taken together, XIST promoted the expression of YY1 by competitively binding to miR-34a-5p.

### XIST regulated AIA-FLS function via miR-34a-5p/YY1 axis

The AIA-FLS were transfected with sh-XIST + inhibitor NC, sh-XIST + miR-34a-5p inhibitor,

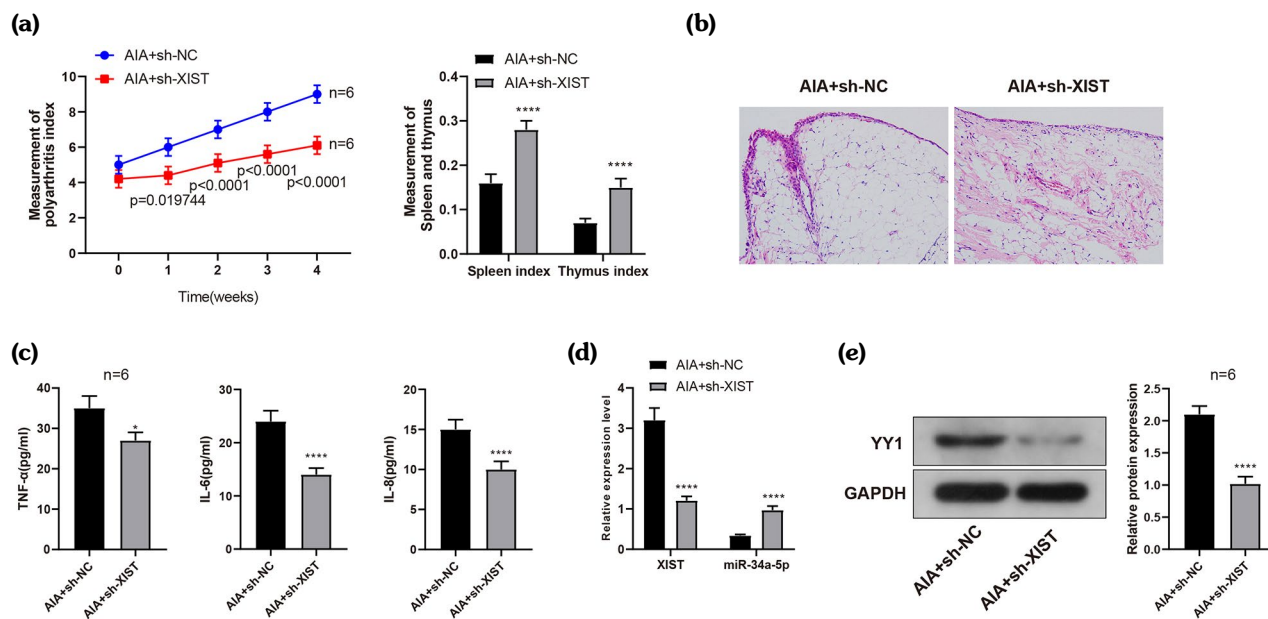


**Figure 5.** Silencing of XIST suppresses AIA in rats via miR-34a-5p/YY1 axis. AIA rats were injected with sh-NC or sh-XIST. **(a)** The polyarthritis, spleen and thymus indexes were used to assess synovial inflammation in AIA rats; two-way analysis of variance was used to determine the p values. **(b)** H&E staining was used to reveal the histopathological changes in synovium. **(c)** ELISA was used to detect the expression of TNF- $\alpha$ , IL-6 and IL-8 in synovial fluid. **(d)** qRT-PCR was to detect the expression of XIST and miR-34a-5p in synovium. **(e)** Western blotting was used to detect YY1 protein in synovium.

XIST: X-inactive specific transcript; \*\*\*\*  $p<0.0001$ , compared with the sh-NC group ( $n=6$  per group). The above measurement data are expressed as mean  $\pm$  standard deviation. Independent samples t-test was performed for comparisons between two groups unless specifically stated; AIA: Adjuvant-induced arthritis; TNF- $\alpha$ : Tumor necrosis factor-alpha; IL: Interleukin; qRT-PCR: Quantitative real-time polymerase chain reaction.

sh-XIST + oe-NC or sh-XIST + oe-YY1 and assigned to different groups according to the transfection. The expression of YY1 was increased in the sh-XIST + miR-34a-5p inhibitor group (*vs.* the sh-XIST + inhibitor NC group,  $p < 0.0001$ ) and sh-XIST + oe-YY1 group (*vs.* the sh-XIST + oe-NC group,  $p < 0.0001$ ) (Figure 4a). The proliferation (Figure 4b,  $p = 0.0023$ ,  $p = 0.0022$ ), migration (Figure 4d,  $p < 0.0001$ ) and invasion (Figure 4e,  $p < 0.0001$ ) of AIA-FLS were promoted, and the apoptosis (Figure 4c,  $p < 0.0001$ ) was inhibited in the sh-XIST + miR-34a-5p inhibitor group (*vs.* the sh-XIST + inhibitor NC group) and sh-XIST + oe-YY1 group (*vs.* the sh-XIST + oe-NC group).

### **Silencing of XIST suppressed AIA in rats via miR-34a-5p/YY1 axis**

The AIA rats were injected with sh-NC or sh-XIST ( $n = 6$  per group). The AIA + sh-XIST group had a lower polyarthritis index ( $p < 0.05$ ) and higher spleen and thymus indexes ( $p < 0.0001$ ) than the AIA + sh-NC group (Figure 5a). The AIA + sh-XIST group showed a reduction in synovial hyperplasia and inflammation compared to the AIA + sh-NC group (Figure 5b). The expression of TNF- $\alpha$ , IL-6 and IL-8 in synovial fluid was decreased in the AIA + sh-XIST group compared to the AIA + sh-NC group (Figure 5c,  $p = 0.0184$ ,  $p < 0.0001$ ,  $p < 0.0001$ ). XIST and YY1 were downregulated and miR-34a-5p was upregulated in the synovium of the AIA + sh-XIST group compared to the AIA + sh-NC group (Figure 5d, e,  $p < 0.0001$ ). The above results indicate silencing of XIST inhibited the procession of AIA via the miR-34a-5p/YY1 axis.

## **DISCUSSION**

Rheumatoid arthritis is an inflammatory arthropathy associated with joint destruction and increased mortality.<sup>27</sup> In healthy joints, FLS lubricate cartilage surfaces by controlling the composition of extracellular matrix and synovial fluid, while RA-FLS are epigenetically imprinted with an aggressive phenotype and secrete pathogenic mediators.<sup>28</sup> Therefore, the disrupted synovial homeostasis in RA can be partially restored by targeting FLS. In this study, we investigated the function of XIST in an AIA rat model and in FLS derived from AIA

rats using gene modification methods. Based on bioinformatics prediction, experiments were designed to validate the relationships between XIST and its downstream targets in AIA-FLS.

The LncRNAs are important epigenetic regulators of RA. LncRNA DILC and lncRNA CASC2-induced apoptosis of RA-FLS by reducing the expression of IL-6 and IL-17, respectively.<sup>29,30</sup> Overexpression of lncRNA GAS5 restrained the proliferation and inflammation of RA-FLS by inhibiting the expression of Sirt1 via miR-222-3p.<sup>31</sup> Downregulation of lncRNA LERFS in RA reduced the binding of hnRNP Q to the mRNAs of genes encoding small GTPase proteins that regulate the motility and proliferation of FLS.<sup>32</sup> LncRNAs have also been found to exhibit regulatory effects on RA in other cell types apart from FLS. To illustrate, lncRNA NEAT1 acted as a positive regulator of Th17 cell differentiation by activating STAT3 protein.<sup>33</sup> Overexpression of lncRNA HOTAIR increased chondrocyte proliferation and reduced Th17 cells by regulating miR-138 and nuclear factor-kappa B (NF- $\kappa$ B) signaling pathway.<sup>34</sup>

The XIST has been intensively studied over the past few decades. It promoted proliferation and inhibited apoptosis in various cancer cells.<sup>35-37</sup> In recent years, the role of XIST in inflammatory conditions has also been identified. It was overexpressed in acute pneumonia and knockdown of XIST inhibited apoptosis and inflammation in LPS-induced lung fibroblasts cells.<sup>38</sup> Upregulation of XIST reduced viability and promoted apoptosis and inflammation of renal cells following ischemia/reperfusion injury.<sup>39</sup> The XIST stimulated NF- $\kappa$ B-dependent inflammation in the adenoids of patients with obstructive sleep apnea/hypopnea syndrome.<sup>40</sup> In this study, we found XIST was highly expressed in the synovium of AIA rats and in AIA-FLS. Silencing of XIST inhibited proliferation, migration, and invasion, and promoted apoptosis in AIA-FLS. Furthermore, silencing of XIST suppressed immune response in AIA rats and reduced inflammatory cell infiltration in the synovium, as well as the production of TNF- $\alpha$ , IL-6 and IL-8.

The miR-34a-5p was identified as a target of XIST. The expression of miR-34a-5p was increased in the synovium of AIA rats injected with sh-XIST. Inhibition of miR-34a-5p restored the function of AIA-FLS with XIST silencing.

A recent study showed that miR-34a released by bone marrow mesenchymal stem cell-derived extracellular vesicles reduced RA inflammation and RA-FLS proliferation by reducing the expression of cyclin I and activating ATM/ATR/p53 signaling pathway.<sup>20</sup> Overexpression of miR-34a-3p arrested the cell cycle of RA-FLS and reduced the production of matrix metalloproteinase-1/9 and pro-inflammatory cytokines.<sup>41</sup> The above evidence suggests that miR-34a negatively regulates the progression of RA in FLS. We further delved into the target gene of miR-34a-5p in AIA-FLS.

The miR-34a-5p bound to the 3'UTR of YY1 mRNA and, therefore, repressed the expression of YY1 protein. The YY1 was downregulated in the synovium of AIA rats with XIST silencing. Overexpression of YY1 improved the function of AIA-FLS in the presence of sh-XIST. The function of YY1 in RA has already been reported by several studies. Knockdown of YY1 ameliorated the severity of arthritis and joint destruction by reducing Th17 cells via inactivation of STAT3.<sup>42</sup> The YY1 interference also reduced neutrophil infiltration and IL-8 production in a collagen-induced arthritis model.<sup>43</sup> The lncRNA NEAT1 promoted the aggressive phenotype and inhibited apoptosis in RA-FLS by increasing the expression of YY1 via miR-410-3p.<sup>44</sup>

In conclusion, XIST promotes the function of AIA-FLS and the progression of AIA via the miR-34a-5p/YY1 axis. This study indicates that XIST may play a significant role in RA and reveals a novel molecular axis in the pathogenesis of AIA. The XIST-based strategies may bring benefit to FLS-targeting therapies for RA. However, AIA rat model may not well mimic RA and there is no clinical data supporting the findings of this study. Therefore, the results should be interpreted with caution. Future research could probe the feasibility of targeting XIST in clinical treatment of RA.

**Ethics Committee Approval:** All animal experiments were carried out under the approval from the Ethics Committee of Shenzhen Futian Hospital for Rheumatic Diseases and followed the regulations for experiment animal use set by the committee as well as the Guidelines for the Care and Use of Laboratory Animals issued by the National Institutes of Health (ethical approval number: FS202002002). The study was conducted in accordance with the principles of the Declaration of Helsinki.

**Data Sharing Statement:** The data that support the findings of this study are available from the corresponding author upon reasonable request.

**Author Contributions:** Conceived the ideas, provided critical materials, supervised the study: W.Y.Z., Y.Z.Z.; Designed the experiments, analyzed the data: W.Y.Z., Y.Z.Z., D.L.P.; Performed the experiments: W.Y.Z., Y.Z.Z., D.L.P. D.Y.Q.; Wrote the manuscript: W.Y.Z., D.L.P., D.Y.Q.; All the authors have read and approved the final version for publication.

**Conflict of Interest:** The authors declared no conflicts of interest with respect to the authorship and/or publication of this article.

**Funding:** This research was funded by commonweal research project in public health of Futian District, Shenzhen in 2020 (project no.: FTWS2020052).

## REFERENCES

1. Sparks JA. Rheumatoid arthritis. *Ann Intern Med* 2019;170:ITC1-ITC16.
2. Firestein GS, McInnes IB. Immunopathogenesis of rheumatoid arthritis. *Immunity* 2017;46:183-96.
3. Favalli EG, Biggioggero M, Crotti C, Becciolini A, Raimondo MG, Meroni PL. Sex and management of rheumatoid arthritis. *Clin Rev Allergy Immunol* 2019;56:333-45.
4. Blum A, Adawi M. Rheumatoid arthritis (RA) and cardiovascular disease. *Autoimmun Rev* 2019;18:679-90.
5. DeQuattro K, Imboden JB. Neurologic manifestations of rheumatoid arthritis. *Rheum Dis Clin North Am* 2017;43:561-71.
6. Spagnolo P, Lee JS, Sverzellati N, Rossi G, Cottin V. The lung in rheumatoid arthritis: Focus on interstitial lung disease. *Arthritis Rheumatol* 2018;70:1544-54.
7. Aletaha D, Smolen JS. Diagnosis and management of rheumatoid arthritis: A review. *JAMA* 2018;320:1360-72.
8. Cheung TT, McInnes IB. Future therapeutic targets in rheumatoid arthritis? *Semin Immunopathol* 2017;39:487-500.
9. Qian X, Zhao J, Yeung PY, Zhang QC, Kwok CK. Revealing lncRNA structures and interactions by sequencing-based approaches. *Trends Biochem Sci* 2019;44:33-52.
10. Bi X, Guo XH, Mo BY, Wang ML, Luo XQ, Chen YX, et al. lncRNA PICSAR promotes cell proliferation, migration and invasion of fibroblast-like synoviocytes by sponging miRNA-4701-5p in rheumatoid arthritis. *EBioMedicine* 2019;50:408-20.
11. Bartok B, Firestein GS. Fibroblast-like synoviocytes: Key effector cells in rheumatoid arthritis. *Immunol Rev* 2010;233:233-55.

12. Wang ZQ, Xiu DH, Jiang JL, Liu GF. Long non-coding RNA XIST binding to let-7c-5p contributes to rheumatoid arthritis through its effects on proliferation and differentiation of osteoblasts via regulation of STAT3. *J Clin Lab Anal* 2020;34:e23496.
13. Dykes IM, Emanuelli C. Transcriptional and post-transcriptional gene regulation by long non-coding RNA. *Genomics Proteomics Bioinformatics* 2017;15:177-86.
14. Lu TX, Rothenberg ME. MicroRNA. *J Allergy Clin Immunol* 2018;141:1202-7.
15. Lin J, He Y, Chen J, Zeng Z, Yang B, Ou Q. A critical role of transcription factor YY1 in rheumatoid arthritis by regulation of interleukin-6. *J Autoimmun* 2017;77:67-75.
16. Wang Y, Jiao T, Fu W, Zhao S, Yang L, Xu N, et al. miR-410-3p regulates proliferation and apoptosis of fibroblast-like synoviocytes by targeting YY1 in rheumatoid arthritis. *Biomed Pharmacother* 2019;119:109426.
17. Xu XP, Peng XQ, Yin XM, Liu Y, Shi ZY. miR-34a-5p suppresses the invasion and metastasis of liver cancer by targeting the transcription factor YY1 to mediate MYCT1 upregulation. *Acta Histochem* 2020;122:151576.
18. Song AF, Kang L, Wang YF, Wang M. MiR-34a-5p inhibits fibroblast-like synoviocytes proliferation via XBP1. *Eur Rev Med Pharmacol Sci* 2020;24:11675-82.
19. Sun Z, Zhang B, Cui T. Long non-coding RNA XIST exerts oncogenic functions in pancreatic cancer via miR-34a-5p. *Oncol Rep* 2018;39:1591-600.
20. Wu H, Zhou X, Wang X, Cheng W, Hu X, Wang Y, et al. miR-34a in extracellular vesicles from bone marrow mesenchymal stem cells reduces rheumatoid arthritis inflammation via the cyclin I/ATM/ATR/p53 axis. *J Cell Mol Med* 2021;25:1896-910.
21. Fan C, Cui X, Chen S, Huang S, Jiang H. LncRNA LOC100912373 modulates PDK1 expression by sponging miR-17-5p to promote the proliferation of fibroblast-like synoviocytes in rheumatoid arthritis. *Am J Transl Res* 2020;12:7709-23.
22. Charan J, Kantharia ND. How to calculate sample size in animal studies? *J Pharmacol Pharmacother* 2013;4:303-6.
23. Festing MF. Design and statistical methods in studies using animal models of development. *ILAR J* 2006;47:5-14.
24. Festing MF, Altman DG. Guidelines for the design and statistical analysis of experiments using laboratory animals. *ILAR J* 2002;43:244-58.
25. Omolaoye TS, Skosana BT, du Plessis SS. Diabetes mellitus- induction: Effect of different streptozotocin doses on male reproductive parameters. *Acta Histochem* 2018;120:103-9.
26. Livak KJ, Schmittgen TD. Analysis of relative gene expression data using real-time quantitative PCR and the 2(-Delta Delta C(T)) method. *Methods* 2001;25:402-8.
27. van der Woude D, van der Helm-van Mil AHM. Update on the epidemiology, risk factors, and disease outcomes of rheumatoid arthritis. *Best Pract Res Clin Rheumatol* 2018;32:174-87.
28. Nygaard G, Firestein GS. Restoring synovial homeostasis in rheumatoid arthritis by targeting fibroblast-like synoviocytes. *Nat Rev Rheumatol* 2020;16:316-33.
29. Liu C, Guo X, Bai S, Zeng G, Wang H. lncRNA CASC2 downregulation participates in rheumatoid arthritis, and CASC2 overexpression promotes the apoptosis of fibroblast-like synoviocytes by downregulating IL-17. *Mol Med Rep* 2020;21:2131-7.
30. Wang G, Tang L, Zhang X, Li Y. LncRNA DILC participates in rheumatoid arthritis by inducing apoptosis of fibroblast-like synoviocytes and down-regulating IL-6. *Biosci Rep* 2019;39:BSR20182374.
31. Yang Z, Lin SD, Zhan F, Liu Y, Zhan YW. LncRNA GAS5 alleviates rheumatoid arthritis through regulating miR-222-3p/Sirt1 signalling axis. *Autoimmunity* 2021;54:13-22.
32. Zou Y, Xu S, Xiao Y, Qiu Q, Shi M, Wang J, et al. Long noncoding RNA LERFS negatively regulates rheumatoid synovial aggression and proliferation. *J Clin Invest* 2018;128:4510-24.
33. Shui X, Chen S, Lin J, Kong J, Zhou C, Wu J. Knockdown of lncRNA NEAT1 inhibits Th17/CD4+ T cell differentiation through reducing the STAT3 protein level. *J Cell Physiol* 2019;234:22477-84.
34. Zhang HJ, Wei QF, Wang SJ, Zhang HJ, Zhang XY, Geng Q, et al. LncRNA HOTAIR alleviates rheumatoid arthritis by targeting miR-138 and inactivating NF-κB pathway. *Int Immunopharmacol* 2017;50:283-90.
35. Cheng Z, Luo C, Guo Z. LncRNA-XIST/microRNA-126 sponge mediates cell proliferation and glucose metabolism through the IRS1/PI3K/Akt pathway in glioma. *J Cell Biochem* 2020;121:2170-83.
36. Hai B, Pan X, Du C, Mao T, Jia F, Liu Y, et al. LncRNA XIST promotes growth of human chordoma cells by regulating miR-124-3p/iASPP pathway. *Oncotargets Ther* 2020;13:4755-65.
37. Liu J, Yao L, Zhang M, Jiang J, Yang M, Wang Y. Downregulation of LncRNA-XIST inhibited development of non-small cell lung cancer by activating miR-335/SOD2/ROS signal pathway mediated pyroptotic cell death. *Aging (Albany NY)* 2019;11:7830-46.
38. Zhang Y, Zhu Y, Gao G, Zhou Z. Knockdown XIST alleviates LPS-induced WI-38 cell apoptosis and inflammation injury via targeting miR-370-3p/TLR4 in acute pneumonia. *Cell Biochem Funct* 2019;37:348-58.
39. Chen F, Hu Y, Xie Y, Zhao Z, Ma L, Li Z, et al. Total glucosides of paeony alleviate cell apoptosis and inflammation by targeting the long noncoding

- RNA XIST/MicroRNA-124-3p/ITGB1 axis in renal ischemia/reperfusion injury. *Mediators Inflamm* 2020;2020:8869511.
40. Zhou Z, Ni H, Li Y, Jiang B. LncRNA XIST promotes inflammation by downregulating GR $\alpha$  expression in the adenoids of children with OSAHS. *Exp Ther Med* 2021;21:500.
41. Hou C, Wang D, Zhang L. MicroRNA-34a-3p inhibits proliferation of rheumatoid arthritis fibroblast-like synoviocytes. *Mol Med Rep* 2019;20:2563-70.
42. Kwon JE, Lee SY, Seo HB, Moon YM, Ryu JG, Jung KA, et al. YinYang1 deficiency ameliorates joint inflammation in a murine model of rheumatoid arthritis by modulating Th17 cell activation. *Immunol Lett* 2018;197:63-9.
43. Lin J, He Y, Wang B, Xun Z, Chen S, Zeng Z, et al. Blocking of YY1 reduce neutrophil infiltration by inhibiting IL-8 production via the PI3K-Akt-mTOR signaling pathway in rheumatoid arthritis. *Clin Exp Immunol* 2019;195:226-36.
44. Wang Y, Hou L, Yuan X, Xu N, Zhao S, Yang L, et al. LncRNA NEAT1 targets fibroblast-like synoviocytes in rheumatoid arthritis via the miR-410-3p/YY1 axis. *Front Immunol* 2020;11:1975.